# pH- and Temperature-Sensitive Microfiltration Membranes from Blends of Poly(vinylidene fluoride)-*graft*-Poly(4-vinylpyridine) and Poly(*N*-isopropylacrylamide)

**Guangqun Zhai**

*Department of Materials Science and Engineering, Jiangsu Polytechnic University, Changzhou, 213016, People's Republic of China*

Received 10 December 2004; accepted 27 June 2005
DOI 10.1002/app.23286
Published online in Wiley InterScience (www.interscience.wiley.com).

**ABSTRACT:** The copolymer poly(vinylidene fluoride)-*graft*-poly(4-vinylpyridine) (PVDF-*g*-P4VP) was prepared through the graft copolymerization of poly(vinylidene fluoride) with 4-vinylpyridine. Through the blending of the PVDF-*g*-P4VP copolymer with poly(*N*-isopropylacrylamide) (PNIPAm) in an *N*-methyl-2-pyrrolidone solution, PVDF-*g*-P4VP/PNIPAm membranes were fabricated by phase inversion in aqueous media. Elemental analyses indicated that the blend concentration of PNIPAm in the blend membranes increased with an increase in the blend ratio used in the casting solution. Scanning electron microscopy revealed that the membrane surface tended to corrugate at a low PNIPAm concentration and transformed into a smooth morphology at a high PNIPAm concentration. The surface morphology and pore size distribution of the microfiltration membranes could be regulated by the blend concentration of the casting solution, temperature, pH, and ionic strength of the coagulation bath. X-ray photoelectron spectroscopy revealed a significant enrichment of PNIPAm on the membrane surface. The flux of aqueous solutions through the blend membranes exhibited a pH- and temperature-dependent behavior. © 2006 Wiley Periodicals, Inc. J Appl Polym Sci 100: 4089–4097, 2006

**Key words:** blends; membranes; stimuli-responsive polymers

## INTRODUCTION

Arising from its excellent chemical inertness and mechanical properties, poly(vinylidene fluoride) (PVDF) has been widely investigated for its applications as membrane materials for ion conduction[1–3] and gas separation[4–8] during the past decades. However, for certain biologically related applications, such as organ-specific drug delivery and hemodiafiltration, polymer membranes are required to be stimuli-responsive.[9] They will undergo changes in their physicochemical properties, for example, hydrophilic–hydrophobic transformation, dissolution and micellization, aggregation and segregation, and isomerization, in response to applied external stimuli, such as the temperature, pH, and irradiation wavelength.[10] Such prerequisites have limited the applications of PVDF membrane in such areas to a certain extent. To overcome such a drawback, a great deal of effort has been undertaken to impart to the existing polymer membranes specific stimuli-responsiveness through the surface graft copolymerization of functional molecules via γ-ray radiation,[11] glow-discharge treatment,[12–14] UV radiation,[15] plasma activation,[16,17] and ion-beam radiation.[18]

Recently, we reported on the strategy of molecular graft copolymerization of PVDF with 4-vinylpyridine (4VP) side chains [the copolymer poly(vinylidene fluoride)-*graft*-poly(4-vinylpyridine) (PVDF-*g*-P4VP)] before microfiltration (MF) membrane fabrication by phase inversion.[19] The preparation of pH-sensitive MF membranes from the PVDF-*g*-P4VP copolymers by phase inversion has greatly facilitated the control of the pore size, the pore size distribution, and the composition of the pore surfaces by adjusting the casting conditions. In this work, we report on the fabrication of MF membranes from blends of the PVDF-*g*-P4VP copolymer and poly(*N*-isopropylacrylamide) (PNIPAm). Such MF membranes exhibit both pH-sensitive and thermoresponsive permeability to aqueous solutions.

## EXPERIMENTAL

### Materials and reagents

PVDF (Kynar 761, weight-average molecular weight = 552,000) was obtained from Elf Atochem of North America, Inc. 4VP (95% purity), purchased from Aldrich Chemical Co. (Milwaukee, WI), was distilled

*Correspondence to:* G. Q. Zhai (zhai_gq@hotmail.com).
Contract grant sponsor: Natural Science Foundation of China; contract grant number: 20574033.
Contract grant sponsor: Natural Science Foundation of Jiangsu Province; contract grant number: BK 2005404.

under reduced pressure before use. PNIPAm (weight-average molecular weight = 20,000–25,000) was also purchased from Aldrich Chemical. The solvent, *N*-methyl-2-pyrrolidone (NMP), was obtained from Merck Chemical Co. (Darmstadt, Germany).

### Fabrication of the MF membranes

The MF membranes were prepared by phase inversion. The PVDF-*g*-P4VP copolymer was synthesized as reported previously.[19] The monomer feed ratio, defined as the [4VP]/[—$CH_2CF_2$—] molar ratio and used for the graft copolymerization, was 2.55, and the reaction time was fixed at 3 h. The bulk [N]/[C] ratio of the copolymer so obtained was determined to be 0.025 from elemental analysis. The bulk graft concentration, defined as the number of 4VP repeat units per repeat unit of PVDF, or the $([—4VP—]/[—CH_2CF_2—])_{bulk}$ ratio, was calculated to be 0.06. After filtration and purification, the PVDF-*g*-P4VP copolymer powders were redissolved in NMP. PNIPAm was added to achieve the desirable blend ratio, defined as the number of *N*-isopropylacrylamide (NIPAm) repeat units per repeat unit of PVDF, or the $([—NIPAm—]/([—CH_2CF_2—])_{solution}$ molar ratio. The polymer concentration of the casting solution, on the other hand, was based on the total weight of the polymer blend in the solution. After the complete dissolution, the polymer solution was cast onto a glass plate. The glass plate was subsequently immersed in doubly distilled water. After the membrane had detached from the glass plates, it was extracted into a second bath of doubly distilled water at 70°C for several minutes. The purified MF membrane was dried by vacuum pumping under reduced pressure for the subsequent characterization.

### Membrane characterization

The carbon, nitrogen, and hydrogen elemental contents were determined with a PerkinElmer 2400 element analyzer (Wellesley, MA). Taking into account the stoichiometries of the graft and the fluoropolymer chain, we calculated the bulk graft concentration of the PVDF-*g*-P4VP copolymer from the elemental composition as follows:

$$([—4VP—]/[—CH_2CF_2—])_{bulk} = 2[N]/([C] - 7[N]) \quad (1)$$

where the factors 2 and 7 are introduced to account for the fact that there are 2 and 7 carbon atoms per repeat unit of PVDF and 4VP polymer chains, respectively.

For the PVDF-*g*-P4VP/PNIPAm MF membrane, its $([N]/[C])_{bulk}$ ratio was also determined from elemental analyses. The bulk concentration, or the $([—NIPAm—]/[—CH_2CF_2—])_{bulk}$ ratio, was determined from the $([N]/[C])_{bulk}$ ratio as follows:

$$([—NIPAm—]/[—CH_2CF_2—])_{bulk} = (2([N]/[C]_{bulk}) + 7 \times 0.06 \times ([N]/[C])_{bulk} - 0.06)/(1 - 6 \times ([N]/[C])_{bulk}) \quad (2)$$

where the factors 2, 7, and 6 are introduced to account for the fact that there are 2, 7, and 6 carbon atoms per repeat unit of PVDF, 4VP polymer, and PNIPAm, respectively, whereas 0.06 stands for the bulk graft concentration of the PVDF-*g*-P4VP copolymer used in this study.

The morphology, pore size distribution, and surface composition of the MF membranes were studied by scanning electron microscopy (SEM), liquid-displacement porosimetry, and X-ray photoelectron spectroscopy (XPS), respectively, as reported earlier.[19–21]

### Measurements of the temperature- and pH-dependent flux through the blend membranes

The blend membrane was immersed in an aqueous solution of the prescribed pH and temperature, before being mounted on the MF cell (UHP-25, Toyo Roshi, Tokyo, Japan). An aqueous solution of the same prescribed pH and temperature, at a fixed ionic strength of 0.1 mol/L, was added to the cell. The flux was calculated from the volume of the permeate as a function of time. The MF cell containing the permeate was kept in a thermostated water bath for at least 20 min before the flow was initiated. The permeate temperature was checked by a thermometer installed at the outlet of the filtration cell.

## RESULTS AND DISCUSSION

### Blending of the PVDF-*g*-P4VP copolymer with PNIPAm and fabrication of the PVDF-*g*-P4VP/PNIPAm MF membrane

Details on the synthesis and characterization of the PVDF-*g*-P4VP copolymer have been reported earlier.[19] In this work, elemental analysis was employed to determine the composition of the PVDF-*g*-P4VP copolymer used for blending with PNIPAm, as well as that of the resulting PVDF-*g*-P4VP/PNIPAm MF membranes. The $([N]/[C])_{bulk}$ ratios of the pristine PVDF-*g*-P4VP membrane and the PVDF-*g*-P4VP/PNIPAm MF membranes cast from different solution blend ratios, or the $([—NIPAm—]/[—CH_2CF_2—])_{solution}$ ratios, are compared with the $([N]/[C])_{bulk}$ ratio predetermined when the blend was prepared in the casting solution. Figure 1 indicates that the $([N]/[C])_{bulk}$ ratio and the bulk blend concentration, or the $([—NIPAm—]/[—CH_2CF_2—])_{bulk}$ ratio of the PVDF-*g*-P4VP/PNIPAm MF membrane, increases with an increase in the blend ratio used for membrane fabrication, or the $([—NIPAM—]/([—CH_2CF_2—])_{solution}$ ratio. Figure 1 also suggests that

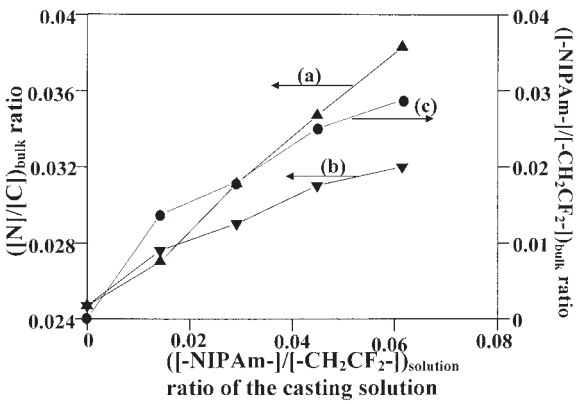


**Figure 1** Dependence of the $([N]/[C])_{bulk}$ ratio and the $([—NIPAm—]/[—CH_2CF_2—])_{bulk}$ ratio of the PVDF-*g*-P4VP/PNIPAm blend membranes on the solution blend ratio: (a) the calculated $([N]/[C])_{bulk}$ ratio, (b) the determined $([N]/[C])_{bulk}$ ratio, and (c) the $([—NIPAm—]/[—CH_2CF_2—])_{bulk}$ ratio.

the $([N]/[C])_{bulk}$ ratio determined from elemental analysis is smaller than the theoretical $([N]/[C])_{bulk}$ ratio calculated from the solution blend ratio, so it can be concluded that part of PNIPAm in the blend solution was extracted into the coagulation bath during the phase-inversion process.

## Surface characteristics of the PVDF-*g*-P4VP/PNIPAm MF membranes

After the PVDF-*g*-P4VP/PNIPAm blend membranes were fabricated, XPS and SEM were used to investigate the variation in the chemical composition and surface morphology, respectively, of the MF membranes.

### Surface morphology of the PVDF-*g*-P4VP/PNIPAm MF membranes

The dependence of the morphology of the MF membranes on the amount of PNIPAm entrapped in the PVDF-*g*-P4VP matrix was investigated with SEM. The SEM images, obtained at a magnification of 5000×, for the MF membranes cast by phase inversion at 25°C from 12 wt % NMP solutions of PVDF-*g*-P4VP and PNIPAm at solution blend ratios of 0.014, 0.029, and 0.061 are shown in Figure 2. The SEM micrographs in

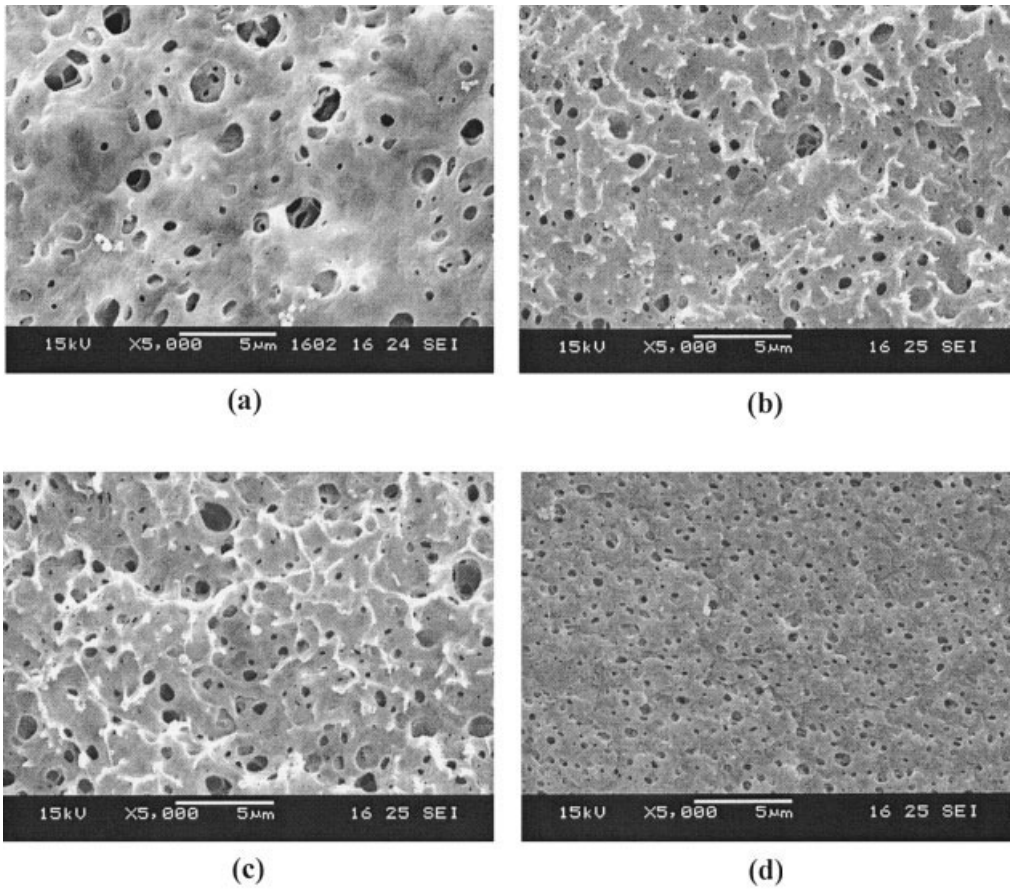


**Figure 2** SEM micrographs of PVDF-*g*-P4VP/PNIPAm MF membranes cast by phase inversion in water (pH 6) at room temperature from 12 wt % NMP solutions of different blend ratios of (a) 0 [PVDF-*g*-P4VP MF membrane, $([N]/[C])_{bulk}$ = 0.025], (b) 0.014 [PVDF-*g*-P4VP/PNIPAm MF membrane, $[N]/[C])_{bulk}$ = 0.027], (c) 0.029 [PVDF-*g*-P4VP/PNIPAm MF membrane, $[N]/[C])_{bulk}$ = 0.029], and (d) 0.061 [PVDF-*g*-P4VP/PNIPAm MF membrane, $[N]/[C])_{bulk}$ = 0.032].

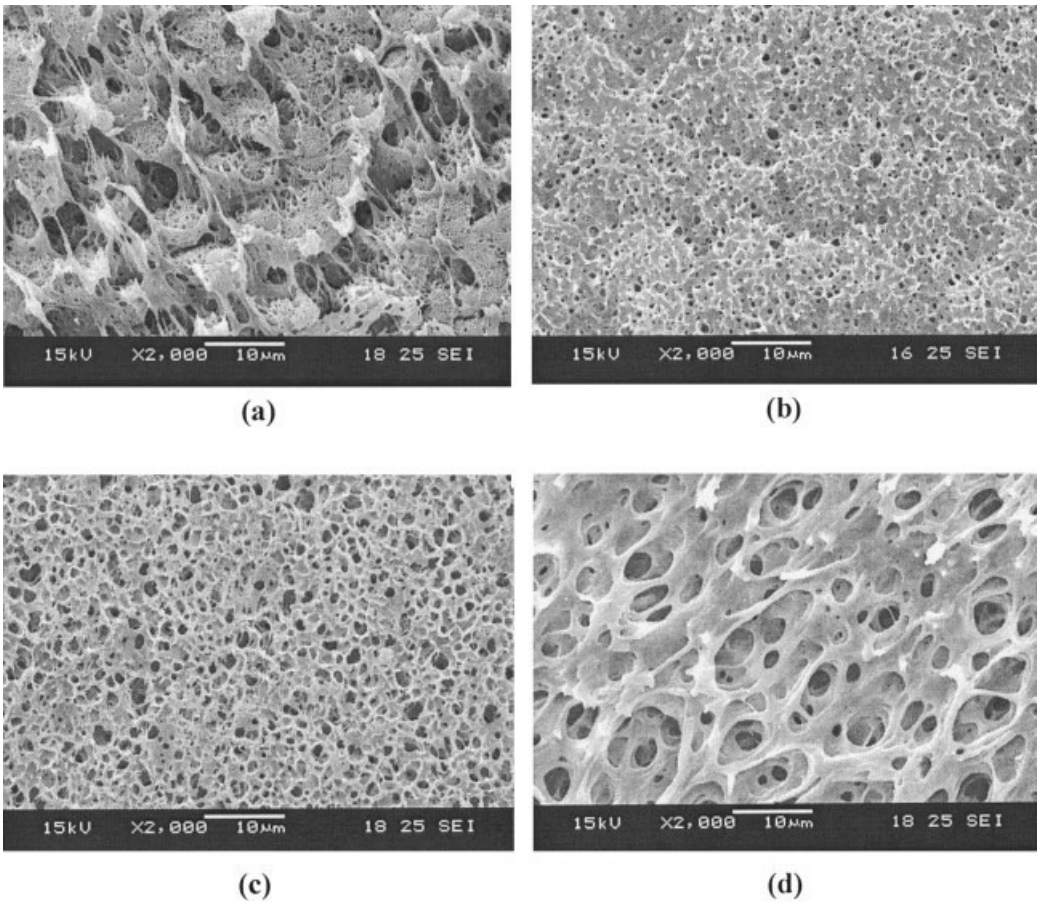


**Figure 3** SEM micrographs of PVDF-*g*-P4VP/PNIPAm MF membranes cast by phase inversion from 12 wt % NMP solutions with a PNIPAm concentration of 0.029 in water (pH 6) at (a) 0, (b) 25, (c) 45, and (d) 70°C.

Figure 3 indicate that the incorporation of PNIPAm into the PVDF-*g*-P4VP matrix gives rise to a decrease in the pore size. This phenomenon is probably associated with the fact that a small pore size can lead to a large specific surface area, arising from the increased interaction of the hydrophilic 4VP and PNIPAm segments at the membrane surface with the aqueous medium during phase inversion. Figure 2 also shows that when the blend ratio is no more than 0.029, the PVDF-*g*-P4VP/PNIPAm MF membranes become corrugated at the surface. At the higher PNIPAm content, the PVDF-*g*-P4VP/PNIPAm MF membrane switches to a smooth morphology.

As a thermoresponsive polymer, PNIPAm can undergo a hydrophilic–hydrophobic transformation at its lower critical solution temperature (LCST) of about 32°C in an aqueous medium. It is water-soluble at room temperature but becomes micellized and forms aggregate when the aqueous medium is heated above its LCST.[9] The effect of the temperature of the casting bath on the morphology of the PVDF-*g*-P4VP/PNIPAm MF membrane was also investigated by SEM. Figure 3 shows the SEM images, obtained at a magnification of 2000×, of the PVDF-*g*-P4VP/PNIPAm MF membranes (blend ratio = 0.029) cast by phase inversion in a coagulation bath at temperatures of 0, 25, 45, and 70°C. The SEM images in Figure 3 clearly suggest that the membranes cast at temperatures below the LCST of PNIPAm have a much smaller pore dimension than those cast at temperatures above 32°C.

The dependence of the surface morphology of the PVDF-*g*-P4VP/PNIPAm MF membranes on the pH value of the coagulation bath was also investigated by SEM. Figure 4 shows the SEM images, obtained at a magnification of 2000×, of the PVDF-*g*-P4VP/PNIPAm MF membranes (blend ratio = 0.061) cast in aqueous media of different pH values (6 and 2) by phase inversion at room temperature. Sodium chloride was added to the bath to fix the ionic strength at 0.1 mol/L. The SEM images in Figure 4 suggest that the MF membrane cast at a lower pH value has a larger pore size than that cast at higher pH values. When membranes are cast in aqueous solutions of different pH values, pyridine rings are involved in various degrees of interaction with the aqueous media. They become positively charged at low pH values. The electrostatic repulsion among the positively charged pyridine groups on the membrane surface

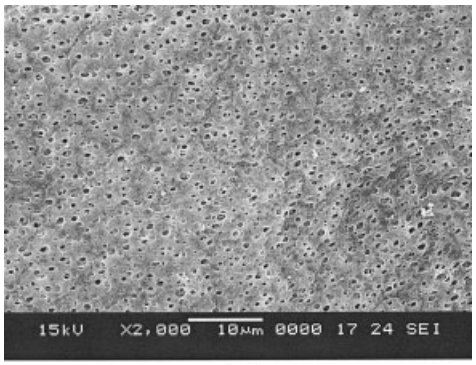


(a)

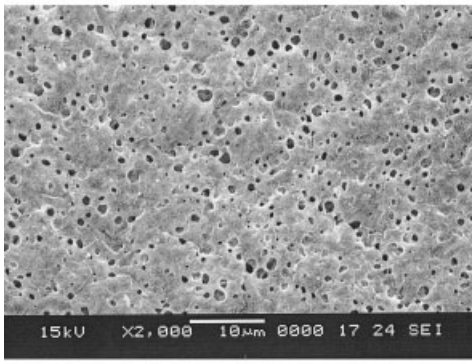


(b)

**Figure 4** SEM micrographs of PVDF-*g*-P4VP/PNIPAm MF membranes cast by phase inversion from 12 wt % NMP solutions [([—NIPAm—]/[—$CH_2CF_2$—]) = 0.061] in water at room temperature (the ionic strength was fixed at 0.1 mol/L) with (a) pH 6 and (b) pH 1.

enhances the pore sizes of the MF membranes when they are cast at the low pH values (high proton concentration).

## XPS analysis of the PVDF-*g*-P4VP/PNIPAm MF membranes

The C 1s core-level spectra of the PVDF-*g*-P4VP/PNIPAm MF membranes cast from 12 wt % NMP solutions of the polymer blends are shown in Figure 5. For the PVDF-*g*-P4VP MF membrane [Fig. 5(a)], the C 1s core-level spectrum can be curve-fitted with four peak components with the following strategy. The peak components of about equal intensities at binding energies (BE) of about 286.0 eV and 290.5 eV are assigned to the $CH_2$ and $CF_2$ species, respectively, of the PVDF main chains of the copolymer. The peak components at the BEs of about 284.6 and 285.8 eV are assigned to the *C*H and *C*N species of the grafted 4VP polymer side chains in the copolymers.[19,21] For the PVDF-*g*-P4VP/PNIPAm MF membranes, the C 1s core-level spectra can be curve-fitted with an approach similar to that of the PVDF-*g*-P4VP membrane. Besides the peak components associated with PVDF-*g*-P4VP, the carbon species at the PNIPAm backbone and the CN species of PNIPAm occur at BEs of about 284.6 and 285.8 eV, respectively, similar to those of the 4VP polymer side chains. In addition to the four peaks mentioned previously, the peak component at a BE value of about 287.4 eV can be assigned to the HN*C*═O species of PNIPAm.[21]

The C 1s core-level spectra in Figure 5 show that, because of the presence of PNIPAm on the membrane surface, the peak intensity of the $CF_2$ species decreases with an increase in the PNIPAm content. The proportion of the $CF_2$ species, determined from the $CF_2$ peak component spectral area, decreases from 27 to 9% when the blend ratio increases from 0 (PVDF-*g*-P4VP MF membrane) to 0.061. On the other hand, Figure 6 also show that the percentage of the HN*C*═O species of the PNIPAm segments, determined in a manner similar to that of the $CF_2$ species, increases gradually from 0 to 7.5% when the blend ratio increases from 0 to 0.061.

The surface blend concentration of PNIPAm on the PVDF-*g*-P4VP/PNIPAm blend membranes, or the $([—NIPAm—]/[—CH_2CF_2—])_{surface}$ ratio, is directly determined from the XPS spectral area ratios of the

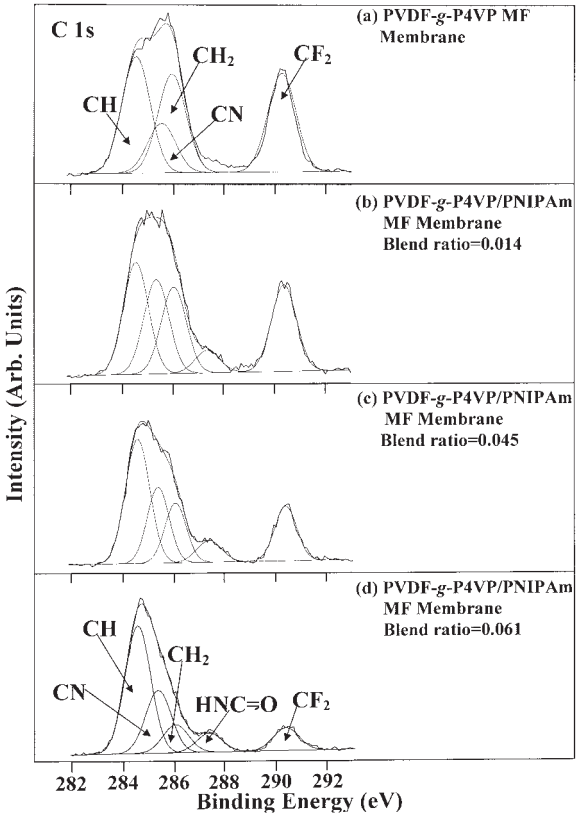


**Figure 5** XPS C 1s core-level spectra of the PVDF-*g*-P4VP/PNIAPm MF membranes cast by phase inversion in water at room temperature from 12 wt % NMP solutions of different blend ratios of (a) 0, (b) 0.014, (c) 0.045, and (d) 0.061

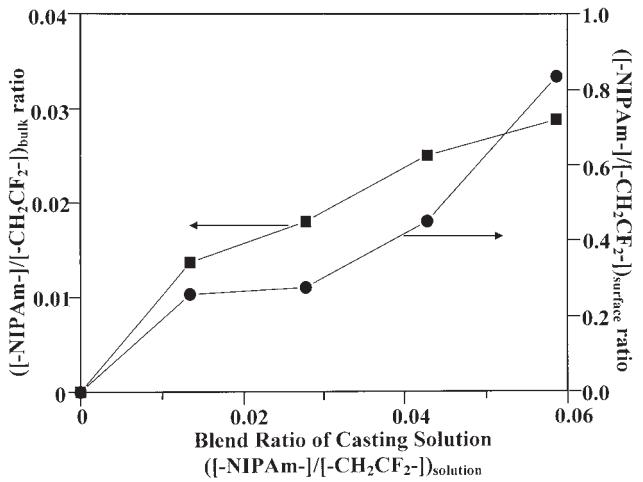


**Figure 6** Dependence of the surface and bulk [—NIPAm—]/[—$CH_2CF_2$—] molar ratio of the PVDF-*g*-P4VP/PNIPAm blend membranes on the blend (molar) ratio for the membrane casting solution ([—NIPAm—]/[—$CH_2CF_2$—]$_{solution}$).

HNC═O species of the PNIPAm segments and $CF_2$ species of the PVDF backbones. Figure 6 shows a comparison of the bulk and surface blend concentrations of the PVDF-*g*-P4VP/PNIPAm membranes cast from solutions of different blend ratios. It is unambiguous that although both the bulk blend concentration and the bulk concentration increase with an increase in the solution blend ratio, the surface concentration is an order of magnitude higher than the bulk concentration. Although such a surface enrichment of PNIPAm chains has been observed in MF membranes,[21] it occurs much more significantly in the PVDF-*g*-P4VP/PNIPAm blend membrane than in the MF membrane prepared from PVDF with PNIPAm side chains (the PNIPAm-*g*-PVDF copolymer). It probably results from the fact that, in comparison with the grafted PNIPAm side chains, the hydrophilic PNIPAm homopolymers are much less hindered during the migration from the polymer matrix to the membrane surface to maximize the interfacial interaction with the aqueous media during the phase-inversion process.

## Pore size of the PVDF-*g*-P4VP/PNIPAm MF membranes

The pore sizes of the PVDF-*g*-P4VP/PNIPAm MF membranes cast under various conditions, such as the polymer solution concentration, pH value, temperature, and ionic strength of the coagulation bath, were measured on a Coulter Porometer II apparatus (Buckinghamshire, UK) with the commercial liquid Porofil as the wetting agent, as reported previously.[19–21]

The average pore sizes of the various PVDF-*g*-P4VP/PNIPAm MF membranes cast from the polymer solution in NMP (blend ratio = 0.029) in casting baths of different pH values are shown in Table I.

**TABLE I**
**Pore Size Distribution of the PVDF-*g*-P4VP/PNIPAm MF Membranes**

| Blend ratio | pH value of the casting Bath | Temperature of the casting bath | Ionic strength of the casting bath (mol/L) | Concentration of the casting solution | Minimum pore size ($\mu$m) | Maximum pore size ($\mu$m) | Mean pore size ($\mu$m) |
|---|---|---|---|---|---|---|---|
| Effect of the pH value of the casting bath on the pore size distribution[a] | | | | | | | |
| 0.029 | 6 | 25 | 0.1 | 12 wt % | 0.20 | 2.33 | 1.15 |
| 0.029 | 4 | 25 | 0.1 | 12 wt % | 0.23 | 3.62 | 1.23 |
| 0.029 | 3 | 25 | 0.1 | 12 wt % | 0.23 | 3.18 | 1.45 |
| 0.029 | 2 | 25 | 0.1 | 12 wt % | 0.84 | 2.89 | 1.51 |
| 0.029 | 1 | 25 | 0.1 | 12 wt % | 0.50 | 3.18 | 1.67 |
| Effect of the temperature of the casting bath on the pore-size distribution[b] | | | | | | | |
| 0.029 | 6 | 0 | 0 | 12 wt % | 0.73 | 2.56 | 1.21 |
| 0.029 | 6 | 25 | 0 | 12 wt % | 0.35 | 2.85 | 1.35 |
| 0.029 | 6 | 45 | 0 | 12 wt % | 0.29 | 3.18 | 1.90 |
| 0.029 | 6 | 70 | 0 | 12 wt % | 1.48 | 5.00 | 2.36 |
| Effect of the ionic strength of the casting bath on the pore-size distribution[a] | | | | | | | |
| 0.029 | 1 | 25 | 0.1 | 12 wt % | 0.50 | 3.18 | 1.67 |
| 0.029 | 1 | 25 | 0.3 | 12 wt % | 0.20 | 1.84 | 0.96 |
| 0.029 | 1 | 25 | 0.5 | 12 wt % | 0.66 | 1.84 | 0.92 |
| 0.029 | 1 | 25 | 0.7 | 12 wt % | 0.20 | 1.52 | 0.71 |
| 0.029 | 1 | 25 | 1 | 12 wt % | 0.25 | 1.72 | 0.67 |
| Effect of the polymer concentration on the pore size distribution[b] | | | | | | | |
| 0.061 | 6 | 25 | 0 | 10% | 0.23 | 5.00 | 1.94 |
| 0.061 | 6 | 25 | 0 | 12% | 0.25 | 1.84 | 0.69 |
| 0.061 | 6 | 25 | 0 | 15% | 0.12 | 0.61 | 0.18 |

[a] Hydrochloride and sodium chloride were added to the casting bath to achieve the desired pH and ionic strength values, respectively.
[b] Cast in doubly distilled water.

Besides the polydispersity in the pore size distribution, the mean pore size of the MF membranes increases with an increase in the proton concentration (decrease in the pH value) of the casting bath. The pyridine rings interact with protons via hydrogen bonding and protonation when the membrane is cast in an aqueous acid solution, and this leads to the formation of the positively charged pyridine groups on the MF membrane surfaces. Because of the electrostatic repulsion among the positively charged pyridine groups on the membrane surface at low pH values of the casting bath, the pore size is enhanced.[19]

The effect of the temperature of the casting bath on the pore size distribution of the MF membrane (blend ratio = 0.029) was also studied. The results are also shown in Table I. Because of the presence of thermoresponsive PNIPAm, the hydrophilic nature of the MF membrane surface decreases with an increase in the temperature of the casting bath during phase inversion, especially when the temperature of the casting bath is greater than 32°C. As a result, a PVDF-*g*-P4VP/PNIPAm MF membrane tends to form a larger specific surface area (smaller pore size) when cast in a bath at lower temperatures than that at a higher temperature.[21]

The dependence of the pore size distribution of PVDF-*g*-P4VP/PNIPAm MF membranes (blend ratio = 0.029) on the ionic strength of the casting bath is shown in Table I. The mean pore size of the MF membranes decreases with an increase in the ionic strength of the casting bath in the presence of a high proton concentration (pH = 1). Our previous studies have shown that most pyridine rings can be protonated to form pyridinium cations when they interact with an aqueous solution of pH 1. The neutral 4VP polymer side chains are transformed into the positively charged polyelectrolyte side chains to some extent.[19,22] In a casting bath of a low ionic strength (0.1 mol/L), the electrostatic repulsion among the positively charged pyridine rings maximizes the pore dimension to reduce the repulsion. For casting in a bath of a high ionic strength, such electrostatic repulsion is shielded by the cations (hydrogen ions and sodium ions) and anions (chloride ions) dissolved in the casting bath (the so-called polyelectrolyte effect). As a result, the mean pore size is reduced because of the decrease in the electrostatic repulsion.[9,22]

The pore size of the PVDF-*g*-P4VPF/PNIPAm MF membranes is also dependent on the copolymer concentration of the casting solution, as shown in Table I. The pore size decreases drastically with an increase in the polymer concentration of the casting solution. At a low polymer concentration, the extraction of the solvent from the bulk matrix, and thus the polymer–solvent phase separation, are facilitated. As a result, larger pore sizes are obtained for the MF membranes cast from copolymer solutions of lower concentrations. The pore size measurement results of the PVDF-*g*-P4VP MF membranes also indicate that the pore size distribution of the PVDF-*g*-P4VP/PNIPAm MF membranes is between those of commercially available hydrophilic PVDF MF membranes with standard pore sizes of 0.45 and 0.65 $\mu$m. Thus, these two commercial PVDF MF membranes are used for a comparative study of the flux behavior of aqueous solutions through PVDF-*g*-P4VP/PNIPAm MF membranes in the latter part of this work.

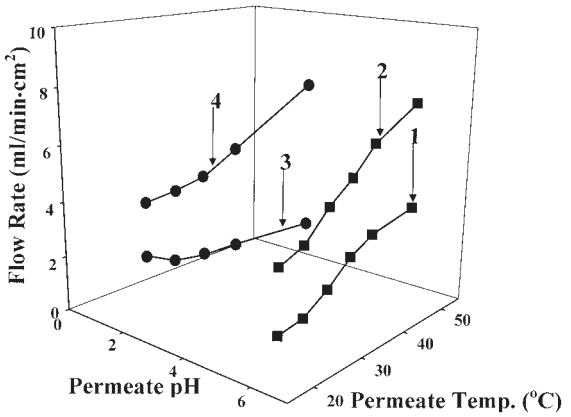


**Figure 7** pH- and temperature-dependent flux behavior of aqueous solutions through the PVDF-*g*-P4VP/PNIPAm blend membranes. Curves 1 and 2 were obtained from PVDF-*g*-P4VP/PNIPAm blend membranes [([—NIPAm—]/[—$CH_2CF_2$—]$_{bulk}$) = 0.061 and 0.029, respectively]. Curves 3 and 4 were obtained from blend membranes [([—NIPAm—]/[—$CH_2CF_2$—]$_{bulk}$) = 0.061 and 0.029, respectively]. Curves 3 and 4 were from the fluxes through the PVDF-*g*-P4VP/PNIAPm MF membrane [([—NIPAm—]/[—$CH_2CF_2$—]) = 0.045 and 0.014, respectively].

### Stimuli-responsive permeability of aqueous solutions through the PVDF-*g*-P4VP/PNIPAm MF membranes

The simultaneous pH- and temperature-dependent flow rates of aqueous solutions through the PVDF-*g*-P4VP/PNIPAm blend membranes are shown in Figure 7. The imposed pressures to achieve such flow rates are 0.03 kg/cm$^2$ for curve 1, 0.06 kg/cm$^2$ for curve 2, 0.03 kg/cm$^2$ for curve 3, and 0.20 kg/cm$^2$ for curve 4. The PVDF-*g*-P4VP/PNIPAm blend membranes exhibit an increase in the permeation rate in response to the increase in the permeate temperature. The temperature-dependent permeation rate probably resulted from the change in the conformation of the PNIPAm polymer on the surface (including the pore surfaces) and subsurface of the blend membrane. At a permeate temperature below the LCST of the PNIPAm polymer, the PNIPAm polymer is hydrophilic. Thus, the PNIPAm chains assume an extended conformation on the surface and in the near-surface regions of the pores, reducing the permeation rate of the aqueous solution. On the other hand, at permeate temperatures

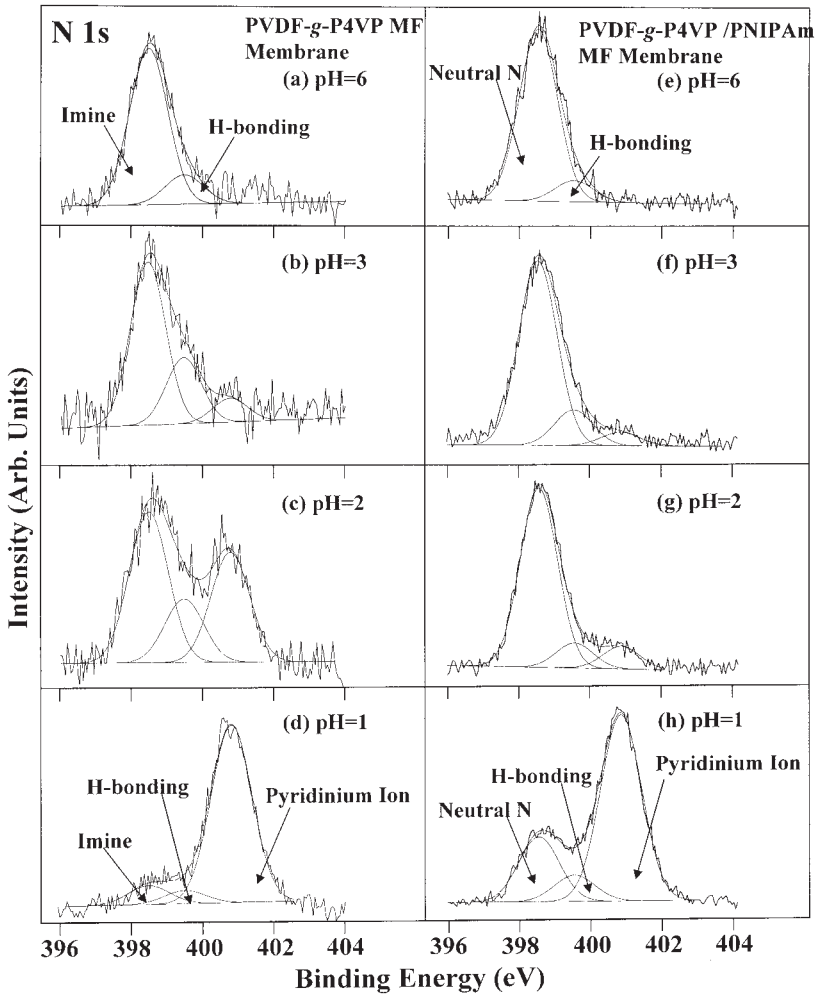


**Figure 8** XPS N 1s core-level spectra of the PVDF-*g*-P4VP MF membrane and PVDF-*g*-P4VP/PNIPAm MF membrane [([—NIPAm—]/[—$CH_2CF_2$—]) = 0.029] after being immersed for 10 min in aqueous solutions of different pH values.

above the LCST, the PNIPAm polymer chains associate hydrophobically on the membrane pore surface and near-surface regions, and this results in the opening of the pores of the membrane and hence the observed increase in the permeation rate.

The changes in the permeation rate of the blend membranes in response to the changes in the permeate pH were attributed to the change in the conformation of the grafted 4VP side chains of the PVDF-*g*-P4VP/PNIPAm blend membrane.[23] The pyridine group can become protonated at a low pH, and this leads to electrostatic repulsion among the charged pyridine groups. The 4VP side chains are forced to switch from the coiled conformation to an extended one, and this results in a decrease in the effective pore dimension and thus the permeability to aqueous media of a low pH.

### pH-induced transition in the chemical states on pyridine nitrogen

To elucidate the process and mechanism underlying the stimuli-responsive permeability of the PVDF-*g*-P4VP/PNIPAm MF membranes to permeate pH, XPS was employed to investigate the variation in the chemical states. The MF membranes were passed through by aqueous solutions of different pH values for 10 min and dried under a reduced vacuum, and the N 1s XPS core-level spectra of the resulting PVDF-*g*-P4VP and PVDF-*g*-P4VP/PNIPAm MF membranes are shown in Figure 8. Nonvolatile perchloric acid ($HClO_4$) and sodium chloride were added to the aqueous solutions to achieve the desired pH value and to fix the ionic strength at 0.1*M*, respectively. Previous studies have suggested that the pyridine ring can be involved in two kinds of specific interaction, that is, protonation and hydrogen bonding, with water, acid, and amide species in aqueous media.[19,24–26] Thus, the XPS N 1s core-level spectra were curve-fitted with three components with the following approach. The main peak component at about 398.5 eV was assigned to the neutral nitrogen (amine of the pyridine rings and amide of PNIPAm).[19,27] The peak component at about 399.5 eV was assigned to the hydrogen-bonded

nitrogen species,[19,28] and the peak component at about 400.8 eV was assigned to the protonated pyridinium ions.[19,29]

The N 1s core-level spectra in Figure 8 clearly indicate that, when the proton concentration is low, or when the pH value is higher than 2, the main form of specific interactions is hydrogen bonding. For the PVDF-*g*-P4VP and PVDF-*g*-P4VP/PNIPAm MF membranes, protonation becomes significant only when the pH value is reduced to 2 and 1, respectively. On the other hand, in comparison with the PVDF-*g*-P4VP MF membrane, the PVDF-*g*-P4VP/PNIPAm exhibits a less strong interaction with an aqueous acid solution of the same pH value. Different from that of the PVDF-*g*-P4VP MF membrane, the nitrogen species of the PVDF-*g*-P4VP/PNIPAm MF membrane surface is composed of the tertiary amine of the pyridine rings and the primary amide of PNIPAm. Because of its extremely weak acidic nature, the nitrogen of the amide cannot be protonated in an aqueous acid solution. Hydrogen bonding is the only interaction with the aqueous solution, leading to a reduced interaction and thus a reduced magnitude of pH sensitivity in the flux behavior of the aqueous solution through the PVDF-*g*-P4VP/PNIPAm MF membrane.

## CONCLUSIONS

Through the blending of the PVDF-*g*-P4VP copolymer and PNIPAm homopolymer in NMP, PVDF-*g*-P4VP/PNIPAm MF membranes were fabricated by phase inversion in aqueous media. Elemental analyses and XPS suggested that the bulk and surface PNIPAm contents increased with an increase in the blend ratio of PNIPAm. SEM and pore size measurements showed that the pore size could be increased with an increase in the temperature and pH value of the casting bath and a decrease in the PNIPAm content, ionic strength of the casting bath, and polymer concentration of the cast solution. The permeation rate of the PVDF-*g*-P4VP/PNIPAm MF membranes increased with an increase in the pH value and temperature of the aqueous solution, and the magnitude of the pH sensitivity of the PVDF-*g*-P4VP MF membrane was compromised by the temperature sensitivity by PNIPAm entrapment. XPS revealed that the pH sensitivity of the MF membranes was reduced by the weakened interaction of the membrane surface with the aqueous acidic media. Such a strategy proposes a convenient approach to fabricating multistimuli-responsive MF membranes.

## References


1. Kataoka, H.; Saito, Y.; Sakai, T.; Quartarone, E.; Mustarelli, P. J Phys Chem B 2000, 104, 11460.
2. Wang, Y.; Travas-Sejdic, J.; Steiner, R. Solid State Ionics 2002, 148, 443.
3. Holmberg, S.; Holmlund, P.; Wilen, C. E.; Kallio, T.; Sundholm, G.; Sundholm, F. J Polym Sci Part A: Polym Chem 2002, 40, 591.
4. Hietala, S.; Skou, E.; Sundholm, F. Polymer 1999, 40, 5567.
5. Yeow, M. L.; Field, R. W.; Li, K.; Teo, W. K. J Membr Sci 2002, 203, 137.
6. Khayet, M.; Feng, C. Y.; Khulbe, K. C.; Matsuura, T. Polymer 2002, 43, 3879.
7. Li, K. Chem Eng Technol 2002, 25, 203.
8. Kong, L. F.; Li, K. J Appl Polym Sci 2001, 81, 1643.
9. Brophy, P. D.; Mottes, T. A.; Kudelka, T. L.; Mcbryde, K. D.; Gradner, J. J.; Maxwold, N. J.; Bunchman, T. E. Am J Kidney Dis 2001, 38, 173.
10. McCormick, C. L. Stimuli-Responsive Water Soluble and Amphiphilic Polymers; American Chemical Society: Washington, DC, 2000.
11. Mazzei, R.; Smolko, E.; Tadey, D.; Gizzi, L. Nucl Instrum Methods B 2000, 170, 419.
12. Ito, Y. Kobunshi Ronbunshu 1998, 55, 171.
13. Ito, Y.; Park, Y. S.; Imanishi, Y. Macromol Rapid Commun 1997, 18, 221.
14. Ito, Y.; Ochiai, Y.; Park, Y. S.; Imanishi, Y. J Am Chem Soc 1997, 119, 1619.
15. Ulbricht, M. React Funct Polym 1996, 31, 165.
16. Lee, Y. M.; Shim, I. K. J Appl Polym Sci 1996, 61, 1245.
17. Lee, Y. M.; Shim, J. K. Polymer 1997, 38, 1227.
18. Omichi, H. Nucl Instrum Methods B 1995, 105, 302.
19. Zhai, G. Q.; Ying, L.; Kang, E. T.; Neoh, K. G. J Mater Chem 2002, 12, 3508.
20. Ying, L.; Wang, P.; Kang, E. T.; Neoh, K. G. Macromolecules 2002, 35, 673.
21. Ying, L.; Kang, E. T.; Neoh, K. G. Langmuir 2002, 18, 6416.
22. Kee, R. A.; Gauthier, M. Macromolecules 2002, 35, 6526.
23. Tonge, S. R.; Tighe, B. J. Adv Drug Delivery Rev 2001, 53, 109.
24. Kato, E.; Murakami, T. Polymer 2002, 43, 5607.
25. Cai, Z. L.; Reimers, J. R. J Phys Chem A 2002, 106, 8769.
26. Fernandez-Berridi, M. J.; Iruin, J. J.; Irusta, L.; Mercero, J. M.; Ugalde, J. M. J Phys Chem A 2002, 106, 4187.
27. Moulder, J. F.; Stickle, W. F.; Sobol, P. E.; Bomben, K. The Handbook of X-Ray Photoelectron Spectroscopy, 2nd ed.; PerkinElmer: Wellesley, MA, 1992; p 227.
28. Liu, S. Y.; Chan, C. M.; Weng, L. T.; Li, L.; Jiang, M. Macromolecules 2002, 35, 5623.
29. Zhou, X.; Goh, S. H.; Lee, S. Y.; Tan, K. L. Appl Surf Sci 1998, 126, 141.